# Laser-induced instantaneous spectral diffusion in $Tb^{3+}$ compounds as observed in photon-echo experiments

G. K. Liu* and R. L. Cone
*Physics Department, Montana State University, Bozeman, Montana 59717*
(Received 11 October 1989)

We have observed a significant "instantaneous spectral diffusion" phenomenon in photon-echo experiments on $Tb^{3+}$:$LiYF_4$. This laser-induced effect makes observed optical dephasing rates intensity dependent and can also contribute a frequency dependence to the measured rates. A change in the magnetic dipole-dipole interaction between $Tb^{3+}$ echo ions and surrounding $Tb^{3+}$ ions occurs when surrounding ions are excited. This causes an instantaneous shift in the optical frequency of the echo ion that lasts for $T_1 \sim 1$ msec. Frequency shifts caused by the first excitation pulse have no effect on echo rephasing ($T_1 \gg T_2$), but those caused by the second pulse prevent proper echo rephasing. A summary is given of other ion-lattice and ion-ion interactions that can cause similar laser-induced effects in a wide variety of insulating compounds. There is potential for probing the nature of inhomogeneous broadening.

## I. INTRODUCTION

The optical analog of the "instantaneous spectral diffusion" phenomenon of electron-spin resonance has been dramatically observed in photon-echo experiments on the $^7F_6\Gamma_2$-to-$^5D_4\Gamma_1$ transition in 1 at.% $Tb^{3+}$:$LiYF_4$.[1-4] If $\Gamma_0$ is the true homogeneous linewidth and $\Gamma'$ is the contribution of instantaneous spectral diffusion, the "apparent" homogeneous linewidth $\Gamma=\Gamma_0+\Gamma'$ determined from measured photon-echo decays depends linearly on the laser intensity of the second laser pulse (at fixed pulse length) and is independent of the laser intensity of the first laser pulse.[2-4] Changes in the apparent linewidth $\Gamma$ of greater than a factor of 10 have been observed. Even larger changes could be induced in this system under what must be regarded as routine experimental conditions.

This instantaneous spectral diffusion effect arises as follows. When generating echoes, the laser excitations can also cause abrupt long lasting changes in the crystal environment (such as random changes in local magnetic or electric fields). These abrupt changes induce extra dephasing. This effect is a direct analog of the instantaneous diffusion in electron-spin echoes studied by Mims[5] and by Klauder and Anderson.[6] In the spin-echo case, the change in local fields is caused by spin reorientation; the reoriented spins are responsible for generating the spin echoes and also contribute to the local fields thus leading to an artificial or experiment-induced line broadening. Following our initial reports of the laser-induced instantaneous spectral diffusion[1,2] and analysis of these effects[2,3] subsequent experiments by Huang *et al.*[7] and Kroll *et al.*[8] have also shown that instantaneous diffusion can arise from optically induced changes in $Eu^{3+}$ and $Pr^{3+}$ compounds.

To explain our optical experiments, the magnetic dipole-dipole interaction between $Tb^{3+}$ ions has been considered, along with other mechanisms which couple a $Tb^{3+}$ ion to the lattice and to other $Tb^{3+}$ ions.[1-4] In this paper, we use our laser intensity-dependent studies to demonstrate *quantitatively* that a change in magnetic dipole-dipole coupling between an echo ion and surrounding ions occurs when the surrounding ions are excited by an optical excitation pulse. This causes an instantaneous shift in the optical transition frequency of the echo ion and prevents complete rephasing. Interaction mechanisms, which could cause instantaneous diffusion in other rare-earth and transition-metal compounds, are also described in this paper.

The impacts of these observations are significant. The photon-echo technique has been regarded as providing an effective way to measure homogeneous linewidths of optical transitions in the time domain in solids where direct measurements in the frequency domain are obscured by inhomogeneous broadening. Moreover, it has been considered free of potential experimental problems (arising, for example, from laser frequency jitter) which can alter the results of other coherent transient methods such as optical free induction decay or the results of saturation spectroscopy. Our results show that orders of magnitude errors are easily made in photon-echo experiments if excitation conditions are not carefully analyzed. These effects can also cause problems in other optical coherent transient and nonlinear spectroscopic experiments.

Indeed, it was the application of the photon-echo technique to dilute and concentrated $Tb^{3+}$ compounds that initially led us to observe the effect.[1-4] With optical coherent transient techniques having reached an advanced stage of interpretation and utilization in dilute solid systems, it has been our goal to apply such techniques to the study of energy transfer processes and collective relaxation phenomena in stoichiometric compounds where strong interactions can take place between the optically active ions. Such experiments are expected to provide interesting probes of energy-transfer processes, spin diffusion, and fluctuations associated with phase transitions. They are also sensitive to the nature of inhomogeneous broadening and its role in energy-transfer

 

processes; hence, there is potential for finding experiments demonstrating a transition from delocalized to localized states.[1,3,4]

Finally, we may identify opportunities to exploit the instantaneous diffusion phenomenon to gain insight into basic material properties such as inhomogeneous broadening and weak ion-ion interactions. Those opportunities are discussed at the conclusion of the paper.

## II. EXPERIMENTAL APPARATUS AND TECHNIQUES

The layout of the two-pulse photon-echo apparatus is shown in Fig. 1. The system can automatically record photon-echo decays versus pulse separation time. Several special features were developed for these experiments.[9,3]

The two-pulse sequence needed to excite conventional photon echoes was provided by two independent, synchronized, thyratron-triggered nitrogen lasers that pumped two tunable dye lasers. The use of two separate dye lasers avoided problems with beam propagation and crossing, which can occur with hundreds-of-nanosecond or microsecond optical delays. The time delay between the two laser pulses was electronically controlled and could be adjusted manually or scanned by computer with a resolution and long term stability of 1 nsec. Special triggering circuits were developed to achieve low jitter, and slow drift was eliminated using a hybrid optoelectronic feedback system with subnanosecond resolution.[10]

The two Hansch-type dye lasers were operated at peak powers of up to 40 kW. Both lasers could be operated in an etalon-narrowed high-resolution mode with a linewidth of $\sim 0.05\ \mathrm{cm}^{-1}$. Without the etalon in the cavity, the lasers operated with a linewidth of $\sim 0.3\ \mathrm{cm}^{-1}$, a value comparable to the inhomogeneous width of the transition studied here. The laser pulses had a duration of 5 nsec and repetition a rate of 6 Hz.

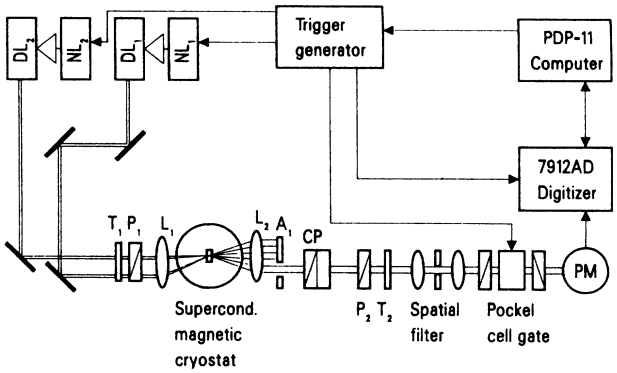


FIG. 1. Apparatus for the photon-echo experiment. Here NL stands for nitrogen laser, DL for dye laser, L for lens, T for half-wave plate, P for prism polarizer, CP for Babinet-Soliel polarization compensator, and A for aperture. The first two polarizers in conjunction with the birefringent sample and compensator form a polarization interferometer that transmits the echo greater than ten times more efficiently than the scattered laser light. A spatial filter made up to two lenses and a pinhole further discriminates the scattered light. Finally two crossed polarizers in conjunction with a Pockels cell made up a shutter for gating the echo to the photomultiplier. A Tektronix transient digitizer records the echo signal.

In addition to measuring the photon echoes, these lasers have been used to record absorption spectra and carry out hole burning experiments in the same sample.[1,11] In the photon-echo experiments the two dye lasers were tuned to the same frequency.

The two dye laser beams were crossed in the sample at their waists. With an $f=1.00$ m lens, the beam diameter was about 200 $\mu$m. A long-focal-length lens was necessary in the photon-echo experiments to keep the power density low because the laser intensity plays a very important role in the echo decay process. A razor blade outside the cryostat was used to locate the beam waist position and to ensure that the two beams crossed at the waist position. By delaying one laser pulse for several tens of microseconds, a laser-induced thermal effect at the sample was also an effective method to adjust the beam focusing and overlap. The sample thickness was chosen to make the absorption about 40% at line center.

The incident laser beams entered the cryostat through a window at the bottom. A superconducting magnet provided fields up to 60 kG. The sample chamber was separate from the magnet helium reservoir, and immersion in superfluid helium allowed cooling the sample below 1.3 K. A Lake Shore CGR-1 resistance thermometer was mounted on the sample holder near the position of the sample. A constant dc current was supplied by a Keithley 227 current source; both the current and the voltage across the element were measured with a four-wire connection.

The transmitted laser beams and the photon echoes were all collected and sent to individual detectors. Polarization discrimination, spatial filtering, and Pockels cell gating were employed to discriminate the echo signal from the laser pulses and scattered laser light. The polarization technique has been discussed in Ref. 9; the first two polarizers in conjunction with the birefringent sample and compensator form a polarization interferometer that transmits the echo greater than ten times more efficiently than the scattered laser light. Other measurements we have made suggest that a discrimination of up to $10^4$ may be achievable.

All of the optical elements for the echo discrimination techniques and the photomultiplier for echo detection were lined up on an optical breadboard, as shown in Fig. 1. The whole breadboard was adjustable with micrometer precision in a direction perpendicular to the beam propagation, providing an optimum arrangement for adjusting the echo detection optics.

The propagation vectors for the laser and the echo beams satisfy the standard echo phase matching condition. In the small-angle crossed-beam geometry used here, the echo was emitted at the same angle relative to the second laser as the second laser was to the first. After the collection lens $L_2$, the three beams were parallel and equally spaced. Since the photon-echo signal was too weak to see, the initial adjustments of all the components were made using the first laser beam. A micrometer translated the entire collection optics breadboard across to the second laser beam and then on to the expected

echo position. After this procedure, no further adjustment was needed during the experiment.

The laser firing and Pockels cell triggering must be exactly synchronized. Computer control[12] of this timing was executed by a homemade fast pulse generator, which produced a sequence of three pulses. The first two pulses were used to trigger the lasers, and the third pulse triggered both the Pockels cell gate and the digitizer that records the echo.

After the Pockels cell gate, a Hamamatsu R928 photomultiplier tube was used to detect the photon echo. These pulses were sent to a fast Tektronix 7912AD transient digitizer. In the digitizer, 512 channels along the time axis can be arbitrarily assigned as signal locations, and the signal can be summed shot by shot. Fifty channels were assigned to the echo. Any drift or background signal level was eliminated on a shot-by-shot basis by subtracting the level obtained from the same number of channels in a region after the assigned signal channels. An IEEE 488 data bus transmitted the data to a PDP-11 computer.[12]

To expand the dynamic range for the echo decay, several neutral density filters were used in front of the photomultiplier to reduce the echo intensity for early delay times. This enabled the echo signal to be recorded over a dynamic range of more than three decades and with pulse separations ranging from 15 nsec to 10 $\mu$sec or longer.

A full echo decay curve was constructed by averaging the signal at an individual fixed delay and then incrementing that fixed delay. The emerging curve was plotted automatically as the experiment proceeded.

## III. MECHANISMS FOR DEPHASING

Dephasing due to normal inhomogeneous broadening is removed by the echo pulse sequence, and thus is not of interest here. Attention in most coherent transient experiments is focused on so-called "homogeneous dephasing" arising from fluctuations in the environment.[13] We consider only the low-temperature limit where phonon interactions are frozen out.

The common homogeneous dephasing mechanisms usually have not been considered to cause intensity-dependent dephasing. As we shall see in the following, however, "quasistatic" laser-induced inhomogeneity arising from the same interactions can occur in the middle of an echo sequence. In that case the effects of the transient laser-induced inhomogeneity are not removed, and "artificial" dephasing occurs.

The effects of concentration are examined in Sec. III A, with emphasis on limiting cases involving isolated ions, low concentrations of interacting ions, and the approach to stoichiometry where rare-earth ion-ion interactions become important. In each of these cases, long-range interactions are important, but in the case of relatively concentrated compounds, short-range interactions can also be important. In Sec. B the general possibilities for coupling a rare-earth ion to the lattice and for coupling a rare-earth ion to other rare-earth ions are examined.

### A. The effects of concentration

In a very dilute rare-earth compound (0.01 at. %), the rare-earth ion-ion interactions are often considered negligible. The excited-state dynamics are then most strongly affected by fluctuations of the local magnetic fields arising from the fluctuating nuclear moments of ligand ions. This situation has been widely studied by many groups, and a recent review has been given by Macfarlane and Shelby.[13]

As the concentration is increased to between 0.1 and 1 at. % or so, ground-state coupling between rare-earth ions can occur. Through the magnetic dipole-dipole interaction, for example, a pair of ions can execute mutual flip flops between the components of their effective spin states. The random distribution of this flip-flop process leads to fluctuations of the local fields which cause homogeneous line broadening. This effect is called spin diffusion, and it naturally gives rise to spectral diffusion.

At approximately the upper end of the concentration range cited in the preceding paragraph (1 at. % level or less), significant rare-earth ion pair coupling can occur due to short-ranged rare-earth ion-ion interactions. Cone and Meltzer[14] and Baker[15] have reviewed both the interaction mechanisms and some of the consequences for level splitting, shifts, and dispersion.

### B. Coupling mechanisms

Table I summarizes the basic interaction mechanisms for a rear-earth ion in a solid. The instantaneous diffusion phenomenon involves the same mechanisms that can cause "true" dephasing, but since it arises from "static" shifts instead of "dynamic" processes, the *diagonal* matrix elements are most important. For that reason, mechanisms that contribute only weakly to dephasing for a particular optical transition could still be important for instantaneous diffusion.[14]

#### *1. Free-ion Hamiltonian*

In general, the excitation of a nearby rare-earth ion could have a small effect on the normal single-ion terms such as electron-electron repulsion and spin-orbit cou-

TABLE I. Interaction mechanisms between a rare-earth ion and the lattice and between two rare-earth ions. (See Ref. 14.)

| | |
|---|---|
| "Free-ion" Hamiltonian terms | |
| Noncentral field | $\sim 10\,000$ cm$^{-1}$ |
| Spin-orbit coupling | $\sim 1000$ cm$^{-1}$ |
| "Weak" crystal field | $\sim 100$–$200$ cm$^{-1}$ |
| Hyperfine, nuclear quadrupole, and transferred hyperfine interactions | $\leq 1$ cm$^{-1}$ |
| Rare-earth–rare-earth interactions | $\leq 10$ cm$^{-1}$ |
| Magnetic dipole-dipole interaction | |
| Electric multipole-multipole interaction | |
| Electronic exchange | |
| Virtual phonon exchange | |

pling. Such effects could arise from local changes in the dielectric constant. Energy shifts of as much as several tens of $cm^{-1}$ have been observed for structurally perturbed sites.[16] Indeed the total inhomogeneous broadening, which at low temperature is often 500–1000 or even 10 000 times the homogeneous broadening in rare-earth compounds, arises from variation of the free-ion and crystal-field interactions combined.

#### 2. *Crystal field*

Excitation of a neighboring ion could change the crystal field for the ion of interest. Evidence of directly measurable energy shifts for closely coupled pairs has been reported by several groups and has been reviewed by Cone and Meltzer.[14] (Separation of the crystal-field effect from other ion-ion interaction effects has remained a problem.) For weaker clusters of ions, these effects would obviously be reduced but could be large enough to be important for the instantaneous diffusion phenomenon where kilohertz level shifts can contribute observable effects.

#### 3. *Hyperfine, nuclear quadrupole, and transferred hyperfine interactions*

These small interactions have played important roles in understanding conventional coherent transient measurements.[13] Certainly in the case of important frozen core effects in the transferred hyperfine interaction, excitation of a nearby ion could modify the coupling between any ion near that core and the surrounding ligand nuclear spins. Modification of the frozen core is a well documented mechanism for hole burning.[13]

#### 4. *Rare-earth–rare-earth interactions*

Rare-earth ion-ion interactions can cause both level shifts (or splittings) and energy-transfer effects. Both can contribute to dephasing. The basic ion-ion interactions listed in Table I have been reviewed by Cone and Meltzer[14] and Baker.[15] It is important to note here that both the magnetic and electric dipole-dipole interactions may be accurately calculated once the dipole moments are measured. Such measurements are straightforward, particularly in the magnetic case. Those two simple interactions may be expected to account for most optically induced frequency shifts in compounds up to about 1% concentration.

In 1 at. % $Tb^{3+}$:$LiYF_4$, the $Tb^{3+}$ ion has a very large magnetic dipole moment,[17,11] so its optical resonant frequency is quite sensitive to the local magnetic field. The magnetic dipole-dipole interaction will be shown to play the dominant role in our system where its calculated effects account for the observed laser-induced dephasing.

## IV. INSTANTANEOUS SPECTRAL DIFFUSION IN $Tb^{3+}$:$LiYF_4$

In electron-spin-echo studies of rare-earth compounds, Mims[5] and Klauder and Anderson[6] pointed out a power-dependent phenomenon called instantaneous spectral diffusion. It arose from the magnetic dipole-dipole interaction. Taylor and Hessler[18] also observed instantaneous spectral diffusion due to the magnetic dipole-dipole interaction in their electron-spin-echo experiments on ruby and postulated[19] that a similar effect in photon-echo experiments on ruby would arise from electric dipole-dipole interactions. Meth and Hartmann,[20] however, observed no intensity-dependent effects for 0.037 at. % $Cr_2O_3$ ruby. Warren and Zewail[21] also considered the possibility of dephasing arising from changes in electric dipole-dipole interactions caused by excited ions. To our knowledge, no observation of instantaneous diffusion effects in photon-echo experiments preceded our initial reports of this effect.[1–3] Subsequent experiments by Huang *et al.*[7] and Kroll *et al.*[8] have shown that the same kind of instantaneous diffusion occurs in $Eu^{3+}$ and $Pr^{3+}$ compounds.

In this Section, we calculate the abrupt changes in local magnetic fields that can be induced by an optical transition. The cumulative effects of excitations throughout the crystal are then evaluated. It is noted that the shift due to the first laser pulse has no effect on echo rephasing when the excited state lifetime $T_1$ is much longer than the pulse delay time $\tau$. On the other hand, those changes caused by the second excitation pulse prevent complete rephasing. This case ($T_1 \gg \tau$) is relevant to most rare-earth transitions. The resulting echo decay rate is independent of the intensity of the first pulse and depends only on the intensity of the second pulse. A quantitative comparison of theory and experiment is made.

### A. Effect of local magnetic fields on optical dephasing

For the optical transitions of ions or molecules in crystals, inhomogeneous broadening includes the effect of any static local electric and magnetic fields and the static interactions between the rare-earth ion and the host lattice. In magnetic compounds such as the $Tb^{3+}$:$LiYF_4$ crystal studied here, the dominant fluctuations in the optical transition energy at low temperature are due to the fluctuating local magnetic fields.[13] The magnetic dipole-dipole interaction[14] thus plays an important role in the homogeneous line broadening.

In 1 at. % $Tb^{3+}$:$LiYF_4$, the $Tb^{3+}$ ion has a very large magnetic dipole moment ($8.85\mu_B$ in the ground state),[11,17] and the changes in local magnetic fields accompanying an optical excitation are dramatic. That interaction is thus the leading candidate to provide the laser-induced frequency shifts responsible for instantaneous diffusion.

### B. Frequency shifts due to the magnetic dipole-dipole interaction

Due to the Zeeman effect in the ground and excited electronic states, an optical frequency is shifted by

$$\Delta\nu_i = [(g_1 - g_2)/2]\mu_B \Delta H/h \ , \tag{1}$$

where $g_1$ and $g_2$ are the $g$ factors for the ground and excited state, respectively, and $\Delta H$ is the total change in the

local field. (The $g$ factors are based on the usual effective spin $\frac{1}{2}$.) Optical excitations caused by the echo-generating pulses change the magnetic moments of the excited ions, and that leads to changes in the local fields for neighboring ions. For the dipole-dipole interaction,[14] the change in local field at site $i$ after the excitation of a neighboring ion at site $j$ is

$$\Delta H_{ij}=(1/h)[(g_1-g_2)/2]\mu_B(1-3\cos^2\theta_{ij})/r_{ij}^3 , \quad (2)$$

where $r_{ij}$ is the distance between sites $i$ and $j$, and $\theta_{ij}$ is the angle between the $z$ direction and the line joining $i$ and $j$. The resonance frequency shift of ion $i$ due to excitation of ion $j$ is then

$$\Delta\nu_{ij}=(1/h)[(g_1-g_2)/2]^2\mu_B^2(1-3\cos^2\theta_{ij})/r_{ij}^3 ,$$

and a sum must be evaluated over the sample, taking into account the random positions of the excited ions.

The frequency shifts due to the first pulse are present throughout the echo-generating sequence and are fixed since $T_1 \gg \tau$ where $\tau$ is the pulse separation. *Their effects are equivalent to those of the normal static inhomogeneous broadening and are removed by the echo sequence.* In contrast, the shifts due to the second pulse are present only for part of the echo sequence, so *their effects are not removed by the rephasing process, and they prevent complete rephasing of the echoes.* In the pseudodipole moment picture, the amount of phase precession of individual dipoles in the dephasing period randomly differs from that in the rephasing period, and the ensemble average of the moments will be reduced.[21]

To evaluate the dephasing rate due to this instantaneous diffusion, the ensemble average of the laser-induced frequency shifts has to be carried out for the crystal lattice. The continuous medium approximation of the lattice is applicable for low concentrations of excited ions and for long-range coupling mechanisms such as the magnetic dipole-dipole interaction. With that approximation,[5] the effect of the instantaneous diffusion is to reduce the echo intensity by

$$I(t)=I_0\exp(-4\tau/T_2') \quad (3)$$

with the decay rate

$$1/T_2'=4\pi^2 J n_e(9/\sqrt{3})=2.53\, J n_e , \quad (4)$$

where $J=[(g_1-g_2)/2]^2\mu_B^2/\hbar$ and $n_e$ is the ion concentration of the sample in the case of an ideal $\pi/2$-$\pi$ pulse sequence.

When the echo-generating pulses are not the ideal $\pi/2$-$\pi$ sequence, for example when $\theta_2<\pi$, the effective number of echo ions will be less than the total number of rare-earth ions in the line, and $n_e$ is no longer the constant ion concentration of the sample.[22] Instead, it will depend on the excitation intensity and the pulse duration $t_d$. That is, $n_e$ becomes the concentration of optical excitations or the excitation density created by the second pulse, and it is an experimental parameter. Suppose a narrow-band laser pulse excites only a small portion of the line. For various choices of laser frequency in the inhomogeneously broadened line, narrow-band echoes can be formed. In such cases, most of the ions in the line make no contribution to the echo. If broader lasers are used, there is a superposition of such effects. When the frequency distributions of two independent laser pulses do not completely overlap, only the overlapping part makes a contribution to the echo, but the entire second pulse makes a contribution to the instantaneous diffusion. In other words, the effective number of ions that cause the instantaneous diffusion depends on the excitation frequency, bandwidth, intensity, and duration of the second pulse.

Basic energy conservation requires the total energy stored in the sample during the excitation to equal the total energy of the excited ions,

$$E_T=\int_\delta \rho(\omega)\hbar\omega d\omega , \quad (5)$$

where

$$N_T=\int_\delta \rho(\omega)d\omega , \quad (6)$$

is the total number of excited ions, $\rho(\omega)$ is the density of excited ions, and $\delta$ is the laser bandwidth. If $\omega_0$ is the center of the inhomogeneous absorption line,

$$E_T=\hbar\omega_0 N_T , \quad (7)$$

since $\omega_0 \gg \delta$. Since that energy is absorbed from the laser pulse,

$$\hbar\omega_0 N_T=t_d A I_2\{1-\exp[-\alpha(\omega)L]\} , \quad (8)$$

where $A$ is the area of the sample exposed to the laser, $L$ is the thickness of the sample, $I_2$ is the intensity of the second pulse, and $\alpha(\omega)$ is the absorption coefficient. For an optically thin sample, the effective concentration can be written as

$$n_e=N_T/AL=(t_d/L\hbar\omega_0)I_2\{1-\exp[-\alpha(\omega)L]\} . \quad (9)$$

From Eq. (4) and (9), the contribution of instantaneous diffusion to the apparent homogeneous linewidth $\Gamma$ is

$$\begin{aligned}\Gamma' &= 1/\pi T_2' \\ &\approx 0.20[(g_1-g_2)^2\mu_B^2/\hbar]n_e \\ &= \frac{0.20(g_1-g_2)^2\mu_B^2 t_d I_2\{1-\exp[-\alpha(\omega)L]\}}{L\hbar^2\omega_0} ,\end{aligned} \quad (10)$$

where $I_2$ is the intensity of the second pulse, $\alpha(\omega)$ is the frequency-dependent absorption coefficient, and $L$ is the optical path length in the crystal. In an exact treatment, the numerical factor 0.20 includes a lattice sum for the dipole-dipole interaction, and it is therefore somewhat crystal-structure dependent and shape dependent. (For further discussion of this point, see Sec. VI.)

### C. Application to $Tb^{3+}$:$LiYF_4$

In our experiments, the echo decays were recorded over 2–3 decades of dynamic range as a function of delay time. A typical decay is shown in Fig. 2. The dephasing rate was very sensitive to the power of the second pulse and also depended on the applied magnetic field as expected.

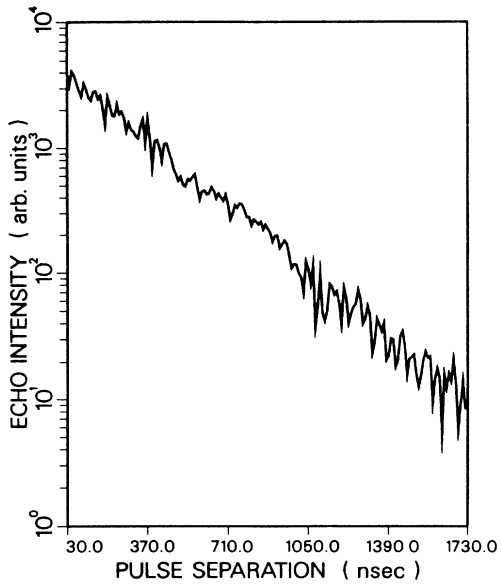


FIG. 2. Typical photon-echo decay curve of $Tb^{3+}$:$LiYF_4$ at 1.3 K showing large dynamic range and exponential decay. The applied magnetic field was 32 kG, and the excitation intensity was 7 MW/cm$^2$. The structure in the decay curve was a reproducible modulation due to transferred hyperfine interactions which are analyzed in Ref. 23. The apparent line width of 285 kHz is much greater than the true homogeneous linewidth. (The reader is cautioned that the 32 kG field used here is different from that used for Fig. 3; the overall decay rate is magnetic field and temperature dependent.)

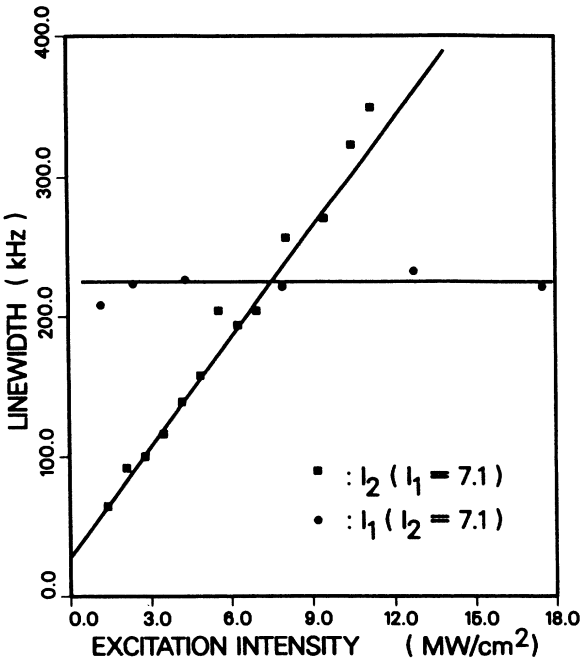


FIG. 3. Excitation intensity dependence of the measured linewidth for $Tb^{3+}$:$LiYF_4$ at 1.3 K. The solid curves are the best fit to the experimental data points. Dephasing only depends on the intensity of the second laser pulse $I_2$. The slope of the curve with $I_2$ varied is 26 kHz/(MW/cm$^2$), and the intersection point is 28 kHz as $I_2$ tends to zero.

Separate studies of echo modulation due to transferred hyperfine interactions with fluorine ligands and of magnetic-field dependence of the dephasing have been carried out[3] on 1 at. % $Tb^{3+}$:$LiYF_4$ and will be reported elsewhere.[23] The modulation, which we have studied in detail, has no effect on the results reported here.

### 1. *Intensity-dependent experiments*

To study the effect of excitation intensity on the dephasing rate of the photon echoes, the peak intensities of the first and second laser pulses were independently varied from 2 to over 15 MW/cm$^2$ by controlling the nitrogen pump laser intensities without any disturbance to the dye laser beam paths or the echo optical system.[3] Figure 3 shows the measured homogeneous linewidth $\Gamma$ as a function of the intensities of the laser pulses at $H=42$ kG and $T=1.3$ K.

The experimental data obey the simple formula predicted by the preceding model

$$\Gamma=\Gamma_0+\Gamma'=\Gamma_0+aI_2 , \tag{11}$$

where $I_2$ is the peak intensity of the second laser pulse on the crystal, $a=26$ kHz/(MW/cm$^2$) is the slope for best fitting the data, and $\Gamma_0=28$ kHz is the true homogeneous linewidth. *At high magnetic field and low temperature, the instantaneous diffusion contribution $\Gamma'$ can clearly dominate the observed echo decay rate.*

The true homogeneous linewidth $\Gamma_0$ includes the contribution from the remaining local field fluctuations due presumably to nuclear-spin diffusion in the applied magnetic field; the ground-state Zeeman splitting is large enough to suppress electron-spin flips. The magnetic field and temperature dependence of the homogeneous linewidth $\Gamma_0$ will be considered in a later paper. We now shift our attention to quantitative determination of the intensity-dependence coefficient $a$.

### 2. *Comparison of theory and experiment for the magnetic dipole-dipole interaction*

The intensity-dependence coefficient $a$ in Eq. (11) is analytically determined by Eq. (10):

$$a=1.26(g_1-g_2)^2\mu_B^2 t_d\{1-\exp[-\alpha(\omega)L]\}/Lh^2\nu_0 . \tag{12}$$

For 1 at. % $Tb^{3+}$:$LiYF_4$ the peak absorption coefficient for this transition is 2.5 cm$^{-1}$. For this sample $L=0.2$ cm, and 40% of the laser power is absorbed at the inhomogeneous line center.[11] In the group of experiments shown in Fig. 3, the laser linewidth was 0.3 cm$^{-1}$, and the inhomogeneous linewidth of the sample was 0.4 cm$^{-1}$. With the assumption of Gaussian line shapes, an average absorption across the inhomogeneous line was then 30% (instead of the 40% applicable in the center of the line). The laser pulse length $t_d=5\times10^{-9}$ sec, and $\nu_0=6.2\times10^{14}$ Hz. The ground state has a linear Zeeman effect with $g_1=17.7$.[11,17] The zero-field eigenfunction of the $^5D_4\Gamma_1$ excited state in the $|M_J\rangle$ representation is

$$|\Gamma_1\rangle=0.42|0\rangle-0.642(|4\rangle+|-4\rangle) , \tag{13}$$

so that state has no first-order Zeeman effect. Due to the coupling to other higher $\Gamma_1$ states in the same multiplet, however, the energy level varies quadratically at low field and asymptotically approaches a linear Zeeman effect at very high field with $g_2=12$. At the 42 kG field relevant to the data of Fig. 3, the effective $g_2$ value is 9.1.[11]

The factors already listed give a calculated value for the intensity-dependence coefficient $a=25$ kHz/(MW/cm$^2$). That value is in agreement with the experimental value of 26 kHz/(MW/cm$^2$) determined from a fit to the data points in Fig. 3. Potential uncertainty in the calculated value arises from the approximation of a continuous medium that was used in the calculation and the uncertainty of various experimental parameters such as the effective diameter of the focused laser beam, laser power loss due to the windows and prisms in the cryostat, and both spatial and frequency overlap of the two laser pulses. The nature of the inhomogeneous broadening can also affect the calculated instantaneous spectral diffusion effects; further discussion of that point is given in Sec. VI.

The electric dipole-dipole interaction is significantly weaker in this compound, so its contribution to the observed instantaneous diffusion may be neglected. It is also quite reasonable to neglect the short-range interactions in this 1% compound at the low excitation densities used in these experiments. The likelihood of having a doubly excited pair is quite small.

We thus conclude that the dominant contribution to the instantaneous diffusion in this case arises from the magnetic dipole-dipole interaction, and that the process is quantitatively understood. Similar analyses may be used when the electric dipole-dipole interaction is important.

## V. EXTENSIONS OF THE BASIC RESULTS

### A. Prediction and observation of frequency dependence

The observed intensity dependence is directly proportional to the excitation density created by the second laser pulse according to Fig. 3 and Eq. (11) and (12). At constant intensity, this excitation-density dependence leads to a frequency dependence, which is directly proportional to the absorption coefficient. (We assume that the sample absorption is not too large.) The predicted frequency dependence has been observed[3] in the 1 at. % $Tb^{3+}$:$LiYF_4$ crystal with the lasers adjusted for narrower bandwidth. The frequency dependence of the echo decay rate due to instantaneous diffusion arises from the excitation of more ions when the lasers are tuned to line center than when they are tuned in the wings. Similar effects have been reported by Huang *et al.*[7] for $Eu^{3+}$:$Y_2O_3$.

### B. Prediction of extreme intensity dependence for pulsed experiments and potential effects in low power experiments

The laser intensities used in Fig. 3 are two orders of magnitude below the damage threshold of approximately 1000 MW/cm$^2$ for this crystal. Extrapolation of Eq. (11) to higher powers predicts extreme intensity dependence for the observed echo decay rates. At 1000 MW/cm$^2$, only 13% of the $Tb^{3+}$ ions are excited, so the linear relationship still holds. The "true" 28 kHz homogeneous linewidth would be increased to 25 MHz, an increase by an amazing factor of 3 orders of magnitude. Under those conditions the apparent dephasing time would be 13 nsec, giving an echo decay time constant for 3.2 nsec. This suggests that echoes would be practically eliminated for intensity conditions routinely used in pulsed laser experiments.[24]

In our initial experiments, a 25 cm lens was used to focus and cross the beams. At an intensity of about 60 MW/cm$^2$, we observed a dephasing time of 200 nsec, a value consistent with our fitted and calculated intensity coefficient $a=25$ kHz/(MW/cm$^2$).

These effects can also be important with low power cw lasers where longer exposure times can still lead to significant excitation during the measurement. The use of heterodyne detection and frequency switching in free-induction-decay or photon-echo experiments is potentially sensitive to these effects.[25] Hole burning linewidths could also be affected.

### C. Observation in $LiTbF_4$

Photon echoes have also been studied in $LiTbF_4$,[1,3,4] where the main goal was to study quasiresonant energy-transfer processes. The echo decay was much faster and had a strong frequency dependence. It was again necessary to carefully extract the intrinsic dephasing rates when obvious effects due to instantaneous diffusion were observed.

### D. Effects in other compounds

Extension of the analysis of Sec. IV to the case of electric dipole-dipole interactions is obvious. That interaction should be particularly important for ions that have singlet electronic states. The reports of instantaneous diffusion for $Eu^{3+}$:$Y_2O_3$ by Huang *et al.*[7] and $Pr^{3+}$:$YAlO_3$ by Kroll *et al.*[8] attribute their observations to an electrostatic mechanism. When the electric dipole moments are measured for those systems, quantitative analysis of the role of electric dipole-dipole interactions can be made.

## VI. PROBING INHOMOGENEOUS BROADENING AND WEAK INTERACTIONS VIA INSTANTANEOUS SPECTRAL DIFFUSION

Because of the important range dependence for any interaction mechanism causing instantaneous spectral diffusion, experiments can be designed to probe the nature of inhomogeneous broadening and possible ion clustering effects in crystals. In the microscopic broadening limit, the spatial variation of optical transition frequency is completely random from site to site, so nearby ions have no correlation in their frequencies. In the macroscopic broadening limit, however, there is a gradual spatial variation of transition frequencies. By using lasers whose bandwidth was less than the inhomogeneous width, and carefully comparing measurements of the intensity coefficient $a$ with Eq. (11), it should be possible to

distinguish the macroscopic broadening case, since the excited ions would be nearer to each other on the average. [Equation (11) implicitly assumes a random distribution.]

In many rare-earth systems, the level shifts due to ion-ion interactions are too weak to be spectrally resolved.[14] Studies of the intensity coefficient $a$ in a variety of systems will provide a new source of data on the systematics of the mechanisms listed in Sec. III. That insight could lead to better models for the interactions and to applications in the analysis of other phenomena.[14]

## VII. OTHER POTENTIAL INTENSITY-DEPENDENT EFFECTS

Among other effects that might give a laser-induced change in the photon-echo decay rate are nonlinear cross relaxation or up-conversion processes such as exciton-exciton annihilation.[14] Such processes are usually described by rate equations with a quadratic or bilinear term in excitation density. They can give rise to dramatic nonlinear changes in the fluorescence decay rate and can contribute to dephasing. We and other groups have looked for dephasing effects due to these processes.[25] We initially considered that mechanism to explain our early observations, but ruled it out for 1 at. % $Tb^{3+}$:$LiYF_4$.[1] Kroll *et al.*[8] recently reported a contribution due to it in $Pr^{3+}$:$YAlO_3$.

## VIII. SUMMARY AND CONCLUSIONS

The experimental results and analysis for 1 at. % $Tb^{3+}$:$LiYF_4$ demonstrate that instantaneous spectral diffusion can play a very important role in the interpretation of homogeneous linewidth measurements via coherent transients or other techniques of nonlinear spectroscopy. The measured photon-echo decay rate for that system was strongly intensity dependent, with the "apparent" homogeneous linewidth changing by a full order of magnitude as the laser intensity was varied over a modest range. Such changes in apparent linewidth can dramatically alter the interpretation of experiments if they are not considered. Indeed, the "true" dephasing rate or linewidth can only be measured by extrapolation to low intensity for the second laser pulse in the echo-generation sequence.

In the case studied here, the laser-induced dephasing effects clearly arose from the static magnetic dipole-dipole interaction. For that interaction and for the formally related electric dipole-dipole case, the effect is largest when the static dipole moments are different for the ground and excited states.

Instantaneous spectral diffusion is important for dilute and concentrated systems. Additional mechanisms may be important in concentrated systems. Instantaneous spectral diffusion offers some interesting opportunities to probe inhomogeneous broadening, which may offset the complications that it introduces to homogeneous linewidth studies.

## ACKNOWLEDGMENTS

This research was supported by National Science Foundation, Montanans on a New Track for Science (NSF/MONTS) and the Research Corporation. We thank H. J. Guggenheim and R. E. Dietz of AT&T Bell Laboratories for providing the 1 at. % $Tb^{3+}$:$LiYF_4$ and $LiTbF_4$ samples used in these experiments.

---

*Present address: Chemistry Division, Argonne National Laboratory, Argonne, IL 60439.

[1]G. K. Liu, M. F. Joubert, R. L. Cone, and B. Jacquier, J. Lumin. **38**, 34 (1987).

[2]R. L. Cone and G. K. Liu, Bull. Am. Phys. Soc. **33**, 676 (1988).

[3]G. K. Liu, Ph.D. thesis, Montana State University, 1988.

[4]G. K. Liu, R. L. Cone, M. F. Joubert, B. Jacquier, and J. L. Skinner, J. Lumin. (to be published).

[5]W. B. Mims, in *Electron Paramagnetic Resonance,* edited by S. Geschwind (Plenum, New York, 1972), pp. 263–351.

[6]J. R. Klauder and P. W. Anderson, Phys. Rev. **125**, 912 (1962).

[7]Jin Huang, J. M. Zhang, A. Lezama, and T. W. Mossberg, Phys. Rev. Lett. **63**, 78 (1989).

[8]S. Kroll, E. Y. Xu, M. K. Kim, M. Mitsunaga, and R. Kachru (unpublished).

[9]Paula Louise Fisher Darejeh, M. S. thesis, Montana State University, 1983; R. L. Cone, Paula Louise Fisher Darejeh, and G. K. Liu (unpublished).

[10]H. L. Carter (private communication).

[11]G. K. Liu, Jin Huang, R. L. Cone, and B. Jacquier, Phys. Rev. B **38**, 11 061 (1988).

[12]Paula L. Fisher and R. L. Cone, Rev. Sci. Instrum. **53**, 634 (1982).

[13]R. M. Macfarlane and R. M. Shelby, in *Spectroscopy of Crystals Containing Rare-Earth Ions,* edited by A. A. Kaplyanskii and R. M. Macfarlane (North-Holland, Amsterdam, 1987), Chap. 3, pp. 51–184.

[14]R. L. Cone and R. S. Meltzer, in *Spectroscopy of Crystals Containing Rare-Earth Ions,* edited by A. A. Kaplyanskii and R. M. Macfarlane (North-Holland, Amsterdam, 1987), Chap. 8, pp. 481–556.

[15]J. M. Baker, Rep. Prog. Phys. **34**, 109 (1971).

[16]R. Faulhaber and S. Hüfner, Z. Phys. **228**, 235 (1969); S. Hüfner, *Optical Spectral of Transparent Rare-Earth Compounds* (Academic, New York, 1978).

[17]I. Laursen and L. M. Holmes, J. Phys. C **7**, 3765 (1974).

[18]D. R. Taylor and J. P. Hessler, Phys. Lett. **50A**, 205 (1974).

[19]D. R. Taylor and J. P. Hessler, Phys. Lett. **53A**, 451 (1975).

[20]S. Meth and S. R. Hartmann, Phys. Lett. **58A**, 192 (1976).

[21]W. S. Warren and A. H. Zewail, J. Phys. Chem. **85**, 2309 (1981); J. Chem. Phys. **78**, 2298 (1983).

[22]That effect was also noted in Refs. 5 and 20.

[23]G. K. Liu and R. L. Cone (unpublished).

[24]The linear relationship breaks down as $\theta$ approaches $\pi$.

[25]R. M. Macfarlane (private communication).